Доклади на Българската академия на науките
Comptes rendus de l'Académie bulgare des Sciences
Tome 78, No 3, 2025

BIOLOGY
Molecular biology

IN SILICO ANALYSIS OF THE INTERACTION OF HUMAN INTERFERON γ C-TERMINAL PEPTIDE AND HEPARAN SULPHATE DERIVED OCTASACCHARIDES

Peicho Petkov[1], Elena Lilkova[1,2]✉, Cvetina Nedeva[1], Leandar Litov[1], Nevena Ilieva[2,3]

Received on February 4, 2025
Presented by I. Ivanov, Member of BAS, on February 25, 2025

Abstract

Human interferon γ (hIFNγ) is a crucial immunomodulatory cytokine that exerts its effects by binding to a high-affinity receptor complex on the cell surface. In addition to receptor binding, hIFNγ also displays strong affinity for heparin and heparan sulphate, primarily via its C-terminal domain. This interaction influences various physicochemical properties of the cytokine, including its receptor affinity, and could be harnessed for designing hIFNγ inhibitors. Current experimental methods cannot precisely determine sulphate group arrangements in heparin-like and HS-like octasaccharides, which influence charge distribution and potentially affect their binding affinity to the hIFNγ C-terminal peptide. Here, we propose an in silico approach to explore different sulphation patterns in octasaccharides containing one acetyl and seven sulphate groups, aiming to identify those that optimize binding to the hIFNγ C-terminal peptide.

Key words: human interferon gamma, heparin, heparan sulphate, molecular interactions, binding affinity, structural design

This work was supported in part by the European Union-NextGenerationEU, through the National Recovery and Resilience Plan of the Republic of Bulgaria, project SUMMIT BG-RRP-2.004-0008-C01. Computational resources were provided by BioSim HPC cluster at the Faculty of Physics, Sofia University "St. Kliment Ohridski" and by the Discoverer supercomputer – Sofia (Bulgaria) thanks to Discoverer PetaSC and EuroHPC JU.

https://doi.org/10.7546/CRABS.2025.03.04

1. Introduction. Human interferon-gamma (hIFNγ) is a critical cytokine essential for immunity against pathogens and tumours, but its excessive or dysregulated activity can drive inflammatory conditions and certain autoimmune diseases [1]. In addition to its cell-surface receptor, hIFNγ also binds strongly to glycosaminoglycans (GAGs) like heparan sulphate (HS) and heparin [2], affecting cytokine stability, distribution, receptor affinity, and proteolytic susceptibility. These GAGs contain highly sulphated NS domains interspersed with lower-sulphation NA regions. hIFNγ preferentially binds to their NS-like regions, with the optimum ligand consisting of two N-sulphated octasaccharides, spaced by an NA-linker. This interaction is mediated by two basic clusters in cytokine's C-terminal region (^{125}KTGKRKR^{131} and ^{137}RGRR^{140}) [2]. Therefore, oligosaccharides engineered to target these clusters can serve as "decoys", inactivating IFNγ before it reaches the receptor and may be helpful in managing autoinflammatory and autoimmune conditions associated with its overproduction [3], such as rheumatoid arthritis, inflammatory bowel disease, and psoriasis, but also viral infections like Covid-19 [4].

Heparin- and HS-derived oligosaccharides are typically produced via enzymatic degradation, where heparinases/heparanases break down natural heparin/HS into oligosaccharides. This cost-effective method enables bulk production but results in heterogeneous mixtures with limited sequence control. Chemoenzymatic synthesis, which combines chemical modifications with glycosyl- and sulphotransferases, allows precise control over sequence, sulphation, and chain length but is 100–1000 times more expensive, making it impractical for large-scale affinity screening.

In this study, we propose an in silico approach to investigate how charge distribution, shaped by different sulphate group arrangements in heparin-like and HS-like octasaccharides, containing one acetyl and seven sulphate groups, affects their binding affinity to hIFNγ C-terminal peptides. Using molecular dynamics (MD) simulations, molecular mechanics with generalized Born and surface area calculations (MM-GBSA), and quasi-harmonic approximation (QHA), we explore various sulphation patterns aiming to identify high-affinity sequences for targeted chemoenzymatic synthesis and experimental validation.

2. Materials and methods. ***2.1. Input structures.*** A total of 35 different octasaccharide sequences (dp8) were used in this study, containing a single N-acetylated glucosamine and seven sulphate groups listed in Table 1. Due to experimental synthesis protocol considerations, the valid monomers are GlcNAc, GlcNAc(6S), GlcNS, GlcNS(6S), IdoA, IdoA(2S), and GlcA. An in-house program was used to generate all possible dp8 sequences which satisfy these requirements. The generation of their structures and CHARMM36-compatible molecular topologies as well as the development of the structural model of the hIFNγ C-terminal peptide with sequence ^{122}AAKTGKRKRSQMLFRGRRASQ^{142} (hIFNγ-CT), is described in detail in [5].

Table 1

Octasaccharides with one acetyl and seven sulphate groups

ID	1	2	3	4	5	6	7	8
1	GlcA	GlcNS	IdoA	GlcNS	IdoA(2S)	GlcNS(6S)	IdoA(2S)	GlcNAc(6S)
2	GlcA	GlcNS	IdoA	GlcNS(6S)	IdoA	GlcNS(6S)	IdoA(2S)	GlcNAc(6S)
3	GlcA	GlcNS	IdoA	GlcNS(6S)	IdoA(2S)	GlcNS	IdoA(2S)	GlcNAc(6S)
4	GlcA	GlcNS	IdoA	GlcNS(6S)	IdoA(2S)	GlcNS(6S)	IdoA	GlcNAc(6S)
5	GlcA	GlcNS	IdoA	GlcNS(6S)	IdoA(2S)	GlcNS(6S)	IdoA(2S)	GlcNAc
6	GlcA	GlcNS	IdoA(2S)	GlcNS	IdoA	GlcNS(6S)	IdoA(2S)	GlcNAc(6S)
7	GlcA	GlcNS	IdoA(2S)	GlcNS	IdoA(2S)	GlcNS	IdoA(2S)	GlcNAc(6S)
8	GlcA	GlcNS	IdoA(2S)	GlcNS	IdoA(2S)	GlcNS(6S)	IdoA	GlcNAc(6S)
9	GlcA	GlcNS	IdoA(2S)	GlcNS	IdoA(2S)	GlcNS(6S)	IdoA(2S)	GlcNAc
10	GlcA	GlcNS	IdoA(2S)	GlcNS(6S)	IdoA	GlcNS	IdoA(2S)	GlcNAc(6S)
11	GlcA	GlcNS	IdoA(2S)	GlcNS(6S)	IdoA	GlcNS(6S)	IdoA	GlcNAc(6S)
12	GlcA	GlcNS	IdoA(2S)	GlcNS(6S)	IdoA	GlcNS(6S)	IdoA(2S)	GlcNAc
13	GlcA	GlcNS	IdoA(2S)	GlcNS(6S)	IdoA(2S)	GlcNS	IdoA	GlcNAc(6S)
14	GlcA	GlcNS	IdoA(2S)	GlcNS(6S)	IdoA(2S)	GlcNS	IdoA(2S)	GlcNAc
15	GlcA	GlcNS	IdoA(2S)	GlcNS(6S)	IdoA(2S)	GlcNS(6S)	IdoA	GlcNAc
16	GlcA	GlcNS(6S)	IdoA	GlcNS	IdoA	GlcNS(6S)	IdoA(2S)	GlcNAc(6S)
17	GlcA	GlcNS(6S)	IdoA	GlcNS	IdoA(2S)	GlcNS	IdoA(2S)	GlcNAc(6S)
18	GlcA	GlcNS(6S)	IdoA	GlcNS	IdoA(2S)	GlcNS(6S)	IdoA	GlcNAc(6S)
19	GlcA	GlcNS(6S)	IdoA	GlcNS	IdoA(2S)	GlcNS(6S)	IdoA(2S)	GlcNAc
20	GlcA	GlcNS(6S)	IdoA	GlcNS(6S)	IdoA	GlcNS	IdoA(2S)	GlcNAc(6S)
21	GlcA	GlcNS(6S)	IdoA	GlcNS(6S)	IdoA	GlcNS(6S)	IdoA	GlcNAc(6S)
22	GlcA	GlcNS(6S)	IdoA	GlcNS(6S)	IdoA	GlcNS(6S)	IdoA(2S)	GlcNAc
23	GlcA	GlcNS(6S)	IdoA	GlcNS(6S)	IdoA(2S)	GlcNS	IdoA	GlcNAc(6S)
24	GlcA	GlcNS(6S)	IdoA	GlcNS(6S)	IdoA(2S)	GlcNS	IdoA(2S)	GlcNAc
25	GlcA	GlcNS(6S)	IdoA	GlcNS(6S)	IdoA(2S)	GlcNS(6S)	IdoA	GlcNAc
26	GlcA	GlcNS(6S)	IdoA(2S)	GlcNS	IdoA	GlcNS	IdoA(2S)	GlcNAc(6S)
27	GlcA	GlcNS(6S)	IdoA(2S)	GlcNS	IdoA	GlcNS(6S)	IdoA	GlcNAc(6S)
28	GlcA	GlcNS(6S)	IdoA(2S)	GlcNS	IdoA	GlcNS(6S)	IdoA(2S)	GlcNAc
29	GlcA	GlcNS(6S)	IdoA(2S)	GlcNS	IdoA(2S)	GlcNS	IdoA	GlcNAc(6S)
30	GlcA	GlcNS(6S)	IdoA(2S)	GlcNS	IdoA(2S)	GlcNS	IdoA(2S)	GlcNAc
31	GlcA	GlcNS(6S)	IdoA(2S)	GlcNS	IdoA(2S)	GlcNS(6S)	IdoA	GlcNAc
32	GlcA	GlcNS(6S)	IdoA(2S)	GlcNS(6S)	IdoA	GlcNS	IdoA	GlcNAc(6S)
33	GlcA	GlcNS(6S)	IdoA(2S)	GlcNS(6S)	IdoA	GlcNS	IdoA(2S)	GlcNAc
34	GlcA	GlcNS(6S)	IdoA(2S)	GlcNS(6S)	IdoA	GlcNS(6S)	IdoA	GlcNAc
35	GlcA	GlcNS(6S)	IdoA(2S)	GlcNS(6S)	IdoA(2S)	GlcNS	IdoA	GlcNAc

For studying the interaction between each pair hIFNγ-CT – dp8 sequence, five distinct initial configurations were prepared to produce varied starting orientations. These input configurations were used to align all 35 octasaccharide sequences, so that for each hIFNγ-CT – dp8 pair the five independent input configurations matched [5]. The resulting systems were subjected to long-scale MD simulations.

2.2. MD simulation protocol. The MD simulation protocol is described in detail in [5]. All MD simulations were carried out using the GROMACS molec-

ular modelling package [6], version 2021.1 and later, with the CHARMM36 force field. Simulations were run under periodic boundary conditions in the isothermal–isobaric (NPT) ensemble at T = 310 K and P = 1 atm. The simulation time was 1 μs for each configuration and trajectory data were saved every 200 ps.

2.3. Estimation of binding free energies. To determine the binding free energy between the peptide and oligosaccharide, we applied the MM-GBSA method combined with QHA. For the MM-GBSA calculations, snapshots were extracted every 0.2 ns from the final 450 ns of each MD simulation, generating 2250 frames per system. The binding free energy ΔG_{bind} was computed using a standard thermodynamic cycle. Polar solvation energy was estimated via the GB-OBC2 model (igb = 5) with a solvent dielectric constant of 78.5 in `gmx_mmpbsa` [7], while nonpolar contributions were derived from SASA using a surface tension parameter of 0.0072.

To estimate entropy changes upon binding, we applied QHA using `gmx_mmpbsa` [7]. A mass-weighted covariance matrix of atomic fluctuations was built from snapshots taken every 0.2 ns over the last 450 ns of each MD trajectory. Prior to analysis, global translational and rotational motions were removed. Diagonalizing this matrix yielded eigenvalues representing quasi-harmonic vibrational modes, which were converted into entropic contributions using statistical mechanics. The final entropy estimate was obtained by averaging over all frames.

3. Results and discussion. We used MD simulations to probe the impact of the charge distribution generated by different sulphate groups arrangements in a series of heparin-like oligosaccharides on their binding affinity towards hIFNγ C-terminal peptides. The net charge per monosaccharide due to a sulphate group substitution can be 0, +1, or +2, as long as the overall net charge of the sulphates sums to +7. Hence, the oligosaccharide sequences from Table 1 can be represented as eight-component vectors denoting the number of sulphate substitutions in each monosaccharide. The enthalpic and entropic contributions to the binding free energy of the investigated complexes obtained from the MD data as described in Section 3.4, are listed in Table 2 and illustrated in Fig. 1.

As seen from these results, for all carbohydrates formation of a complex with hIFNγ-CT is associated with enthalpy gain. The highest enthalpic contribution is exhibited by octasaccharide chains 10, 12 and 4, while the lowest effect of binding on the enthalpy is displayed by chains 29, 31 and 2. On the other hand, while the entropic contribution is almost an order of magnitude smaller than the enthalpic one, its effect is not as unambiguous. For most octasaccharides binding to the peptide is associated with loss of entropy due to reduction in conformational degrees of freedom of the two binding partners. Notably, for chains 2, 20 and 29 binding to the peptide is both enthalpically and entropically favourable. In the investigated systems, no enthalpy–entropy compensation was observed. However, the calculated entropic contributions have significantly larger errors than the

Table 2

Calculated binding free energies of octasaccharides with one acetyl and seven sulphate groups and hIFNGγ-CT

ID	Charge vector	ΔH	err(ΔH)	$-T\Delta S$	err($-T\Delta S$)	ΔG	err(ΔG)
1	01020211	−71.3	1.3	15.1	11.8	−56.2	5.3
2	01021111	−45.7	1.4	−12.0	33.7	−57.7	15.1
3	01021201	−63.3	1.4	9.2	7.0	−54.1	3.2
4	01021210	−79.7	1.5	14.3	4.9	−65.4	2.3
5	01110211	−67.2	1.4	11.5	12.1	−55.8	5.4
6	01111111	−74.9	1.6	8.4	4.9	−66.5	2.3
7	01111201	−68.6	1.5	6.7	13.1	−61.9	5.9
8	01111210	−74.3	1.5	9.7	7.8	−64.6	3.6
9	01120111	−74.4	1.6	2.7	12.8	−71.7	5.8
10	01120201	−81.0	1.4	13.6	3.4	−67.4	1.7
11	01120210	−71.3	1.5	9.9	5.0	−61.4	2.3
12	01121101	−79.8	1.5	6.7	12.1	−73.1	5.5
13	01121110	−74.5	1.5	10.0	4.7	−64.6	2.2
14	01121200	−76.5	1.5	14.4	3.4	−62.1	1.7
15	02010211	−67.0	1.5	5.6	7.0	−61.4	3.2
16	02011111	−69.4	1.4	7.8	7.2	−61.6	3.3
17	02011201	−71.8	1.5	2.5	10.8	−69.3	4.9
18	02011210	−73.4	1.5	12.4	8.9	−61.0	4.0
19	02020111	−67.5	1.5	3.6	19.4	−63.9	8.7
20	02020201	−63.1	1.5	−10.1	21.0	−73.2	9.4
21	02020210	−73.6	1.5	13.7	2.9	−59.9	1.4
22	02021101	−59.7	1.4	1.2	33.2	−58.5	14.9
23	02021110	−75.6	1.4	12.1	6.0	−63.5	2.8
24	02021200	−67.7	1.5	5.3	12.2	−62.4	5.5
25	02110111	−65.0	1.5	3.6	17.7	−61.3	8.0
26	02110201	−63.7	1.5	5.1	16.7	−58.6	7.5
27	02110210	−74.5	1.5	13.0	8.3	−61.4	3.7
28	02111101	−61.8	1.4	9.9	10.7	−51.8	4.8
29	02111110	−56.2	1.4	−2.3	27.6	−58.5	12.3
30	02111200	−69.6	1.5	5.7	5.9	−63.9	2.7
31	02120101	−51.6	1.4	0.0	14.2	−51.5	6.4
32	02120110	−61.1	1.4	3.7	13.1	−57.4	5.9
33	02120200	−74.6	1.4	14.8	4.5	−59.8	2.1
34	02121100	−74.0	1.5	13.3	5.4	−60.7	2.5

enthalpic ones. In particular, octasaccharides that appear to gain entropy upon binding display the largest errors in the respective $T\Delta S$ values.

With the entropic term accounted for, our calculations identify chains 20, 12, 9, 17, and 10 as the top five binders, while chains 31, 28, 3, 5, and 1 exhibit the lowest binding-free-energy values. Notably, chain 20 is among the few outliers with a favourable entropic term and was excluded from the analysis. The two representative samples were augmented with chains 6 and 4, resp. 32, to account properly for the distribution errors. Comparison of the charge vectors (the second

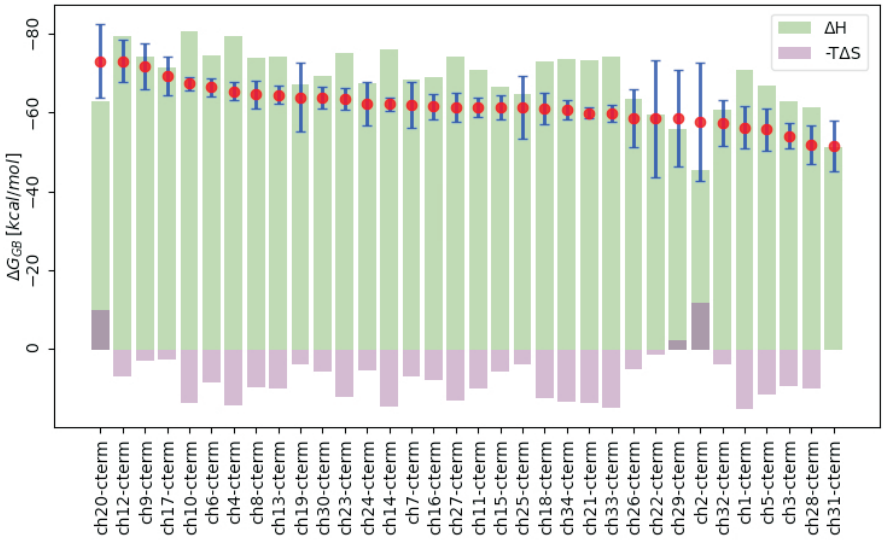

Fig. 1. Binding free energies and their decomposition into enthalpic and entropic contribution of the investigated complexes. Enthalpies are shown in green bars, entropies in purple bars. The resulting free energy values are indicated with red dots and blue error bars, respectively. Octasaccharide chains are ranked in descending order of the estimated ΔG_{bind}

column of Table 2) of these two groups of carbohydrates reveals a pronounced preference of the single substitutions over the double ones at position 2 and a moderate preference for sulphation over non-sulphation on position 5, i.e. N-sulphate at C2 over N-sulphate at C2 and O-sulphate at C6 at position 2, resp. O-sulphate over non-sulphation at position 5.

The observed substitution patterns exhibit moderate yet discernible preferences, likely because the exceptionally high number of sulphate groups — seven within a short octasaccharide chain — blurs stronger trends in the best-performing octasaccharide group in experimental assays. Additionally, both the MM-GBSA and QHA methods have inherent limitations in distinguishing closely related compounds, as seen in this study. MM-GBSA may struggle to capture subtle conformational rearrangements or changes in water structure at the interaction interface, while the purely harmonic nature of QHA can underestimate or mischaracterize entropic changes in the inherently anharmonic motions of biomolecules upon binding. Expanding on the proposed herewith approach — for example, by incorporating multibasin decomposition by root-mean-square deviation clustering [8] prior to the QHA analysis of the MD trajectory [9] – could help overcome the aforementioned limitations, enhance entropy evaluation, and improve binding affinity ranking.

4. Conclusion. Our results demonstrate the potential of combined in silico methods to efficiently survey large oligosaccharide sets, offering initial insights to guide the design and synthesis of hIFNγ inhibitors. In this pilot study, we identified a preferential sulphation pattern — favouring single over double sulphation at position 2 and sulphation over non-sulphation at position 5 — which reduced the octasaccharide set for experimental assays by nearly fivefold.

Acknowledgements. We thank Prof. H. Lortat-Jacob for the experimental data that inspired this study and for the constructive discussions. NI acknowledges the ideas exchange within the COST Action CA21169, supported by COST (European Cooperation in Science and Technology).

REFERENCES

[1] Schroder K., P. J. Hertzog, T. Ravasi, D. A. Hume (2004) Interferon-γ: an overview of signals, mechanisms and functions, J. Leukoc. Biol., **75**(2), 163–189.

[2] Lortat-Jacob H., J. E. Turnbull, J. A. Grimaud (1995) Molecular organization of the interferon γ-binding domain in heparan sulphate, Biochem. J., **310**(2), 497–505.

[3] Vanhaverbeke C., J.-P. Simorre, R. Sadir et al. (2004) NMR characterization of the interaction between the C-terminal domain of interferon-γ and heparin-derived oligosaccharides, Biochem. J., **384**(1), 93–99.

[4] Litov L., P. Petkov, M. Rangelov et al. (2021) Molecular mechanism of the anti-inflammatory action of heparin, Int. J. Mol. Sci., **22**(11), 10730.

[5] Lilkova E., P. Petkov, E. Krachmarova et al. (2025) Modelling the interaction of the hIFNγ C-terminal peptide and HS-derived octasaccharides. In: Advanced Computing in Industrial Mathematics, Volume 522 of Studies in Computational Intelligence, Springer Cham, (in press).

[6] Abraham M. J., T. Murtola, R. Schulz et al. (2015) GROMACS: High performance molecular simulations through multi-level parallelism from laptops to supercomputers, SoftwareX, **1–2**, 19–25.

[7] Valdés-Tresanco M. S., M. E. Valdeés-Tresanco, P. A. Valiente, E. Moreno (2021) gmx_MMPBSA: A new tool to perform end-state free energy calculations with GROMACS, J. Chem. Theory Comput., **17**(10), 6281–6291.

[8] Kenn M., R. Ribarics, N. Ilieva, W. Schreiner (2014) Finding Semirigid Domains in Biomolecules by Clustering Pair-Distance Variations, Biomed Res. Int., **2014**(1), 731325.

[9] Pereira G. P., M. Cecchini (2021) Multibasin Quasi-Harmonic Approach for the Calculation of the Configurational Entropy of Small Molecules in Solution, J. Chem. Theory Comput., **17**(2), 1133–1142.

[1]*Faculty of Physics, Sofia University "St. Kliment Ohridski",*
5 J. Bourchier Blvd, 1164 Sofia Bulgaria
e-mails: peicho@phys.uni-sofia.bg, cvetinanedeva@gmail.com,
Leandar.Litov@cern.ch

[2]*Institute of Information and Communication Technologies,*
Bulgarian Academy of Sciences, Akad. G. Bonchev St, Bl. 25A, 1113 Sofia, Bulgaria
e-mails: elena.lilkova@iict.bas.bg, nevena.ilieva@iict.bas.bg

[3]*Institute of Mathematics and Informatics, Bulgarian Academy of Sciences*
Akad. G. Bonchev St, Bl. 8, 1113 Sofia, Bulgaria